Silicon nano-ribbons on Ag(110): a computational investigation

2010 J. Phys.: Condens. Matter 22 045004

(http://iopscience.iop.org/0953-8984/22/4/045004)

J. Phys.: Condens. Matter **22** (2010) 045004 (5pp) doi:10.1088/0953-8984/22/4/045004

Silicon nano-ribbons on Ag(110): a computational investigation

Abdelkader Kara[1,2,5], Sébastien Vizzini[3], Cristel Leandri[3], Benedicte Ealet[3], Hamid Oughaddou[2,4], Bernard Aufray[3] and Guy LeLay[3]

[1] Department of Physics, University of Central Florida, Orlando, FL 32816, USA
[2] Université de Cergy-Pontoise, LAMAp, 95011 Cergy-Pontoise, France
[3] CINaM-CNRS, Campus de Luminy, Case 913, 13288 Marseille, France
[4] CEA, IRAMIS, SPCSI, 91191 Gif-sur-Yvette, France

E-mail: akara@mail.ucf.edu

Received 11 October 2009, in final form 19 November 2009
Published 5 January 2010
Online at stacks.iop.org/JPhysCM/22/045004

Abstract
We report results of a computational investigation, based on density functional theory, of silicon self-assembled nano-ribbons (Si NRs) on Ag(110). These NRs present a honeycomb-like structure arched on the substrate and forming a closed-packed structure. The calculated STM images match the experimental ones, hinting to a possible new Si structure, mediated by the Ag substrate. The observed new electronic states near the Fermi level were reproduced by the calculations and attributed to a confinement/hybridization tandem.

(Some figures in this article are in colour only in the electronic version)

1. Introduction

Surface alloy formation is generally expected after deposition, at room (or intermediate) temperature, of a thin film on a metallic substrate. Generally, due to the confinement in the surface region, one observes that surface alloys present unusual atomic structures and chemical compositions [1]. From the electronic properties point of view, one category of systems appears particularly interesting: semiconductors-on-metal surfaces. Indeed due to the strong differences of the pure elements, i.e. atomic and electronic structures (metallic bonds versus covalent bonds), one can expect that both strain and confinement might yield novel surface alloying effects. This is especially true for non-reactive metal–semiconductor systems, i.e., systems which present a strong trend toward phase separation. When the trend is toward order, one generally observes the (expected) formation of surface alloys, silicide or germanide like, even though sometimes new interesting superstructures are also observed [2–4].

In the context of systems which show a pronounced tendency toward phase separation, we have already performed studies of the prototype Ge/Ag [5–10] and Si/Ag systems [11–14].

We have recently shown that on Ag(110) the first steps of silicon growth performed at room temperature (RT) reveal the formation of silicon nano-ribbons (NRs) [11], in a massively parallel arrangement along the [$\bar{1}$10] direction of silver. All NRs, that differ only in length (they can reach several tens of nm after soft annealing), present the same widths (1.6 nm) and the same heights (0.2 nm). Low energy electron diffraction (LEED), scanning tunneling microscopy (STM) and high resolution photoelectron spectroscopy using synchrotron radiation (HR-PES-SR) have revealed their perfect chemical order and a strong metallic character [11, 14]. These measurements also revealed new electronic states close to the Fermi level that originally have been attributed to confinement [11]. Furthermore these silicon NRs display a symmetry breaking across their widths, with two chiral species that self-assemble in large left-handed and right-handed domains [14]. Very recently we have also shown that the oxidation process of the Si NRs starts at their extremities and develops like a flame front [12].

To understand the origin of all these specific properties, the knowledge of the atomic and electronic structure of these Si NRs is really of prime importance. Recently we have performed high resolution STM measurements unambiguously showing the hexagonal structure of these NRs. From the theoretical point of view, there is only one study by He [15],

[5] Author to whom any correspondence should be addressed.

who has found various adsorption geometries for Si coverage up to 2 monolayers (MLs). Unfortunately the atomic structure proposed by He does not provide a satisfactory comparison with the experimental data. First this model is based on rectangular symmetry instead of the observed hexagonal one; and second it does not exhibit the symmetry breaking in the $[00\bar{1}]$ direction which is clearly observed experimentally by our STM measurements. For all these reasons it was necessary to reanalyse theoretically the Si NR atomic structure, starting not only from energetic criteria, but also from structural constraints dictated by the new high resolution experimental observation.

This paper is organized as follows: in section 2 computational details will be presented; followed by section 3 detailing the computational results on the atomic and electronic structure; finally, in section 4 we will present our conclusions.

2. Computational details

Ab initio calculations performed in this study are based on density functional theory (DFT) [16, 17]. A comprehensive study of energetics and electronic structure was made by solving the Kohn–Sham equations using the Vienna *ab initio* simulation package (VASP) [18–20]. Exchange–correlation interactions are included within the generalized gradient approximation (GGA) in the Perdew–Burke–Ernzerhof form [21]. The electron–ion interaction is described by the projector augmented wave method in the implementation of Kresse and Joubert [22]. A plane-wave energy cut-off 250 eV was used for all calculations and is found to be sufficient for these systems. The bulk lattice constant for Ag was found to be 0.4175 nm using a k-point mesh of $10 \times 10 \times 10$.

The slab supercell approach with periodic boundaries is employed to model the surface with Brillouin zone sampling based on the technique devised by Monkhorst and Pack [23]. The slab consists of five layers of Ag(110), each containing 24 atoms (4×6). In all our calculations we used a k-points mesh of ($2 \times 3 \times 1$); and the thickness of the vacuum space is about 12 Å. All the results presented in this paper are non-spin-polarized. We do understand that the magnetic solution may differ from the non-magnetic one since the nano-ribbons present chirality, however we believe that spin-polarized calculations will not significantly alter our findings on the structural changes brought to Ag(110) upon Si adsorption and formation of nano-wires. Since the calculated new electronic states are in good agreement with the observed ones, we believe that the magnetic solution will not significantly alter these states. The magnetic properties, absent in the present calculations, are however very important and will be the subject of a subsequent study.

Si nano-ribbons with a variety of geometries (i.e. number of Si atoms) were studied and only the Si30 results are presented in this paper, which was found to match best the experimental structural observations from the STM images, as mentioned above.

3. Results and discussions

Deposition of silicon on Ag(110) at room temperature leads to the growth of silicon nano-ribbons perfectly ordered and aligned along the $[\bar{1}10]$ direction of the silver surface. All these Si NRs present a width of 1.6 nm (i.e. $4a_{Ag[001]}$) and a height of about 0.2 nm, which is evidenced by the line profile along the $[00\bar{1}]$ surface direction. The profile and the 3D STM images revealed the asymmetric shape of these Si NRs in their width [12], with a dip clearly noticeable *only* on the left side of each NR. The STM images also show a transverse asymmetric structure schematically described as a square (side: ∼0.6 nm) joined to a parallelogram. These are the features that will be contrasted with our results from the present computational investigation.

A rigorous determination of the lowest energy configuration of Si nano-ribbons on Ag(110) requires the calculation of all possible arrangements of Si atoms on Ag(110) contained in the surface unit cell. There are two problems with this approach, (i) STM images are not resolved enough to reveal unambiguously the number of Si atoms per unit cell; (ii) even if this number was known, it would be large (30–40 atoms) and a systematic (DFT based) investigation of the total energy for all possible configurations would be very computationally intensive, even impossible in the current situation. We adopt a rather different approach that indeed does not guarantee the lowest energy configuration but yields a possible configuration that complies with a maximum set of constraints imposed by experimental observation. We recall here the most important of these constraints, namely the width of the nano-ribbon covering about four times the lattice constant of Ag, a periodicity along the ribbon of four times the nearest number distance and most importantly, a signature in the STM images of the presence of a square attached to a parallelogram resulting from a unique arrangement of Si NRs on Ag(110). There are several configurations that incorporate the first two constraints, and we will pay more attention to the third constraint to perform the selection. We would like to add here that we found Si atoms tend to form a hexagonal structure even though the substrate here presents a rectangular one. In addition to this, the nature of the bonding between Si atoms is very different from that between Ag atoms and that between Si and Ag atoms. All these properties, coupled with a lattice mismatch between Si and Ag systems, conspire to form a periodic but rather complex structure.

With the above mentioned constraints in mind, we have designed our Ag(110) substrate in such a way to accommodate a large variety of possible Si NRs configurations. The Ag(110) slab consists of five layers, each containing 24 atoms forming six rows containing four atoms each. The choice of five layers was made on the assumption that adsorbed Si NRs might introduce substantial structural perturbations to the substrate. We have studied a large variety of configurations of Si atoms on top of Ag(110), with nano-ribbons containing between 27 and 36 atoms per unit cell. The Si NR starting configurations can be divided in two categories: those in which Si atoms form hexagons and those forming rectangles. Note that in a previous publication, He proposed a configuration where

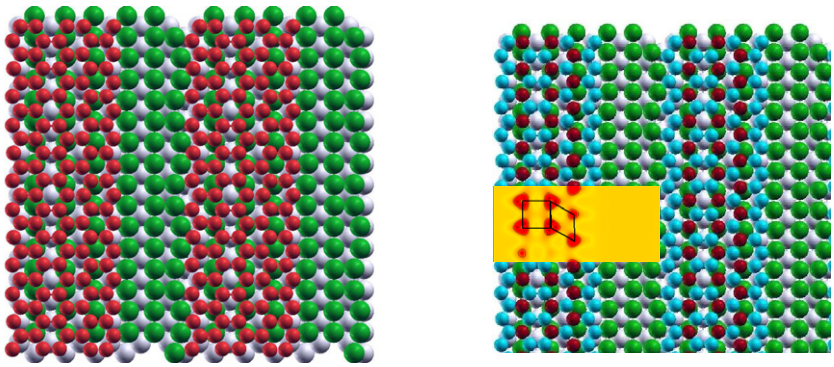

Figure 1. Top view of Si nano-ribbons on Ag(110): (a) silicon atoms (red/dark) forming hexagons along the channels on top of the surface Ag atoms (green); (b) Si atoms sitting at a height 2.7 Å above the Ag surface (red/dark), the inset shows the charge density in a plane just above the silicon ribbon.

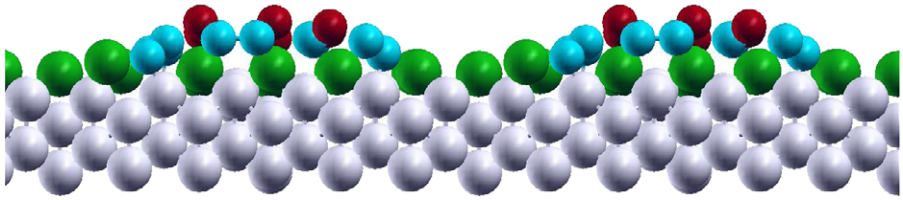

Figure 2. Side view of Si nano-ribbons on Ag(110) showing the arched structure of the ribbons.

dimers of Si atoms formed a rectangular lattice on a 2 × 5 Ag(110) substrate [15]. We have performed calculations for the same configuration on a 4 × 6 Ag(110) substrate. We have found that all the rectangular type configurations experience large deformations upon relaxation, with Si atoms approaching a hexagon structure. The other category of starting configurations consists of silicon nano-ribbons (zigzag type in this study) 4 or 5 hexagons wide adsorbed along the channels of (110). A Si30 configuration would consist of 4 hexagons while a Si36 would consist of 5. As a criterion of selection/elimination, we have used the presence/absence of the STM signature mentioned above (a square adjacent to a parallelogram). In figure 1, we show the top view of the Si30 configuration, with figure 1(a) showing the hexagonal structure that is preserved after full relaxation of the system. After relaxation, the Si ribbon presents strong buckling with the atoms occupying the highest plane shown as red/dark balls in figure 1(b). These atoms form a square attached to a parallelogram and are responsible for the signature seen in the measured STM images (the inset shows the calculated charge density at a plane just above the Si ribbon). Hence, the Si30 structure provides a clear signature of a square attached to a parallelogram, which is absent in the STM images corresponding to other Si configurations.

Let us examine in detail the structural configuration of the Si NR as well as the substrate, before we embark in the analysis of the electronic structure. The width of the ribbon (from the center of the far left Si atom to the center of the far right Si atom) is about 15.1 Å. Since a STM tip does not probe the positions of the center of the atoms, but is rather close to its van der Waals radius, we should add two times the radius of a Si atom to this width in order to compare this value with the experimentally determined one. Since the radius of a Si atom is about 1.2 Å, the apparent width resulting from our calculations would be about 17.5 Å, in excellent agreement with the observed width of about 17–18 Å [8]. As one may notice in figure 2 (a side view of the system), the Si atoms do not sit at the same height, but rather form an arc with a height of 2.06 Å, again in excellent agreement with the experimentally observed one of about 2 Å [8]. The lateral shape of the NR is not symmetric due to the incommensurability, which is also consistent with the experimental observation [8]. This asymmetry is also reflected in the electronic structure of the system. This 'arc-shaped' configuration consists of edge Si atoms penetrating the Ag(110) channels for a better 'grip' onto the surface and a bump due to the Ag rows under the ribbon. As a consequence, the ribbon creates a very interesting corrugation in the charge density profile, as has been reported experimentally [8]. Indeed, at the edges of the Si NRs, there are dips that we will assimilate as 'gutters'. Along the edges of the NRs (along the gutters), the energy profile is weakly corrugated. Hence, one can argue that when Si atoms come from the gas phase or diffuse to the ribbon edge, they are very rapidly dispatched to the ends of the ribbons, contributing to their observed elongation. We believe that it is this 'gutter effect' that is responsible for the formation of very long NRs. This argumentation indeed supposes the formation of a 'seed' configuration forming the first chunks of the gutters. Hence, the present proposed scenario explains how NRs form, but is short from explaining why NRs have a certain well defined

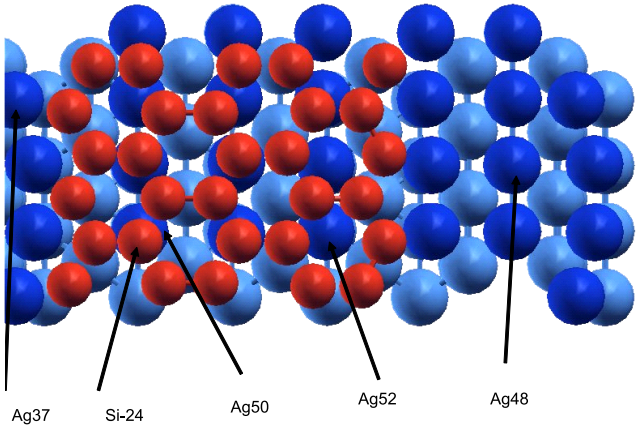

Figure 3. Top view of Si nano-ribbons on Ag(110) showing the labeling of the atoms (used in the text).

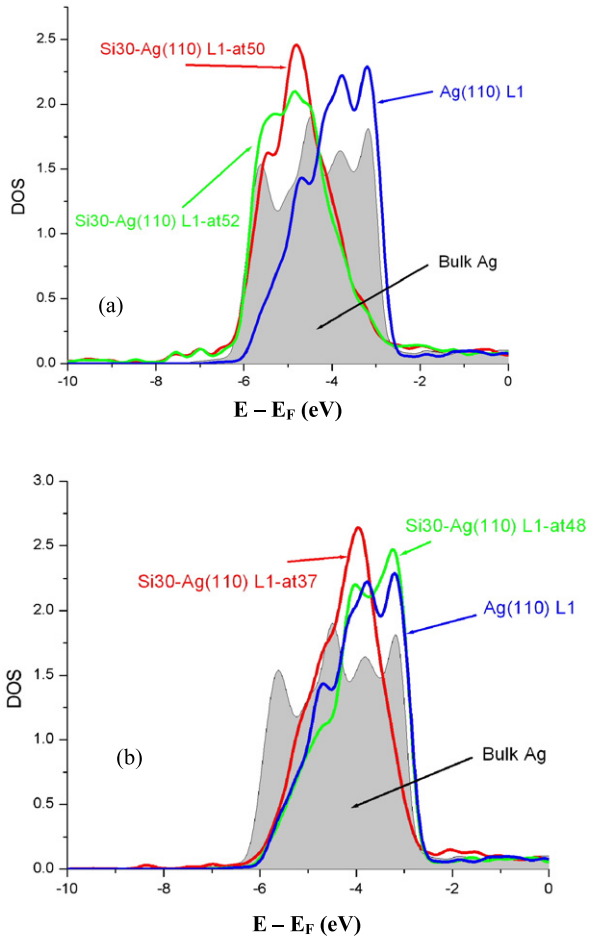

Figure 4. Local density of states for Ag surface atoms as labeled in figure 3 along with those of a surface atom in clean Ag(110) and bulk Ag.

width. We believe that further studies are necessary to answer such a question with confidence.

Let us now turn to the atomic structure of the silver substrate. From figures 1 and 2, one notices that the silver atom chain just on the left of the NR is not straight and presents displacements (of about 0.8 Å) from the ideal position both in and out of the (110) plane. Note that only one side (left) of the ribbon is affected, reflecting again the asymmetric nature of the system as observed experimentally. Not only the positions of atoms on the first layer of the substrate are affected, but also atoms in layers as deep as the 4th layer are different from the ideal ones. Our calculations show that there is a buckling in the 2nd, 3rd, and 4th layers of about 0.6, 0.4 and 0.2 Å, respectively, pointing to a strong bonding between the Si NRs and the Ag substrate. We also found that the chain of silver surface atoms between the NRs (the chain containing atom 48 in figure 3) is not affected. Its atomic, as well as its electronic (as we will show), characteristics are identical to those of the surface atoms of clean Ag(110).

In summary, the Si30 NR relaxes into a configuration that is consistent with several experimental observations regarding the width, height and the asymmetry of the ribbon, which makes this configuration an excellent candidate.

Let us now turn our attention to a local analysis of the electronic structure of these interesting Si NRs. In order to limit our analysis to the most relevant/non-equivalent Ag atoms in the system, we have chosen four different ones, namely atoms 50, 52, 37 and 48 (figure 3), which represent respectively a Ag atom just beneath a Si one, a Ag atom under a hexagon formed by Si atoms, a Ag atom at the edge of the Si ribbon and finally an atom away from the ribbon. In figure 4(a) we show the local density of states for Ag atoms labeled 50 and 52 (both of them under the Si ribbon) along with that of a bulk silver and that of a clean surface atom. Note that the presence of this NR dramatically alters the LDOS of these atoms with a large shift in the top of the d-band away from the Fermi level, by as much as 2 eV. In figure 4(b), we show the LDOS for atoms 37 and 48, respectively at the edge and away from the Si ribbon, along with that of bulk silver and that of a clean surface atom. Note that atoms away (just by one row) from the Si ribbon are not affected at all by the presence of Si atoms whereas the edge atoms band shift away from the Fermi level by about 1 eV with a clear narrowing of the d-band.

In figure 5, we show the LDOS near the Fermi level of silver atoms 50, 52 and 48 along with the LDOS of a Si atom (labeled 24) sitting just on top of atom 50 (as background). We note that the LDOS of atom 50 presents peaks *exactly* at the same position as those of Si-24 revealing a strong *hybridization* between their electronic states. A separate calculation (not shown here) of the electronic structure of a free-standing Si NR of the same structure as Si-30 showed that the peaks mentioned above in the LDOS of Si-24, actually come from a confinement effect. Indeed, the peaks in the LDOS of Si atoms on Ag(110) are at the same position as those of a free-standing NR, allowing us to conclude that the observed new states in the LDOS of Ag atoms are actually due to a tandem of *confinement–hybridization*. These new states are in good agreement with experimental measurements which also revealed new peaks near the Fermi level (around the 2 eV region) in the sp bands and were attributed to a confinement effect [8].

Finally, the Si NR formation energy is determined by calculating the difference in total energy between, on one hand

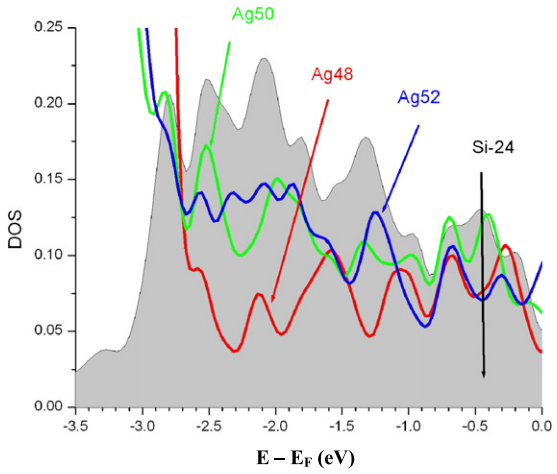

Figure 5. Local density of states for Ag and Si atoms as labeled in figure 3 near the Fermi energy.

Ag(110) and Si NR calculated separately; and Si30/Ag(110) on the other. We found this formation energy to be 0.736 eV per Si atom, reflecting a strong bond between the Si NR and the substrate.

4. Conclusions

We have studied the arrangement of silicon atoms on the Ag(110) surface with an arch-shaped hexagonal configuration that is consistent with the main experimental observations. Furthermore, this hexagonal atomic structure is also in good agreement with the spectroscopic signature of the Si NRs oxidation process, which is very close to the one observed on the Si(111) face [24] (and not to the (001) plane). Finally the calculated new electronic states near the Fermi level are in good agreement with the experimentally observed ones. These new states are attributed to a combination of a confinement (finite lateral size of the ribbons) and a hybridization with the substrate sp states.

Acknowledgments

The work of AK was partially supported by a start-up fund from the University of Central Florida. AK thanks the University of Cergy Pontoise and CINaM-CNRS Marseille for support.

References

[1] Bardi U 1994 *Rep. Prog. Phys.* **57** 939
[2] Polop C, Sacedo'n J L and Martín-Gago J A 1998 *Surf. Sci.* **402–404** 245
[3] Martín-Gago J A *et al* 1997 *Phys. Rev.* B **55** 10896
[4] Polop C *et al* 2001 *Phys. Rev.* B **63** 115414
[5] Oughaddou H, Aufray B, Bibérian J P and Hoarau J Y 1999 *Surf. Sci.* **429** 320
[6] Oughaddou H *et al* 2000 *Phys. Rev.* B **61** 5692
[7] Oughaddou H *et al* 2000 *Phys. Rev.* B **62** 16653
[8] Leandri C *et al* 2004 *Surf. Sci. Lett.* **573** L369
[9] Oughaddou H *et al* 2007 *J. Nanosci. Nanotechnol.* **7** 3189
[10] Oughaddou H *et al* 2008 *Surf. Sci.* **601** 506
[11] Leandri C *et al* 2005 *Surf. Sci. Lett.* **574** L9
[12] De Padova P *et al* 2008 *Nano Lett.* **8** 2299
[13] Leandri C *et al* 2007 *Surf. Sci.* **601** 262
[14] De Padova P *et al* 2008 *Nano Lett.* **8** 271
[15] He G M 2006 *Phys. Rev.* B **73** 035311
[16] Hohenberg P and Kohn W 1964 *Phys. Rev.* **136** B864
[17] Kohn W and Sham L J 1965 *Phys. Rev.* **140** A1133
[18] Kresse G and Hafner J 1993 *Phys. Rev.* B **47** 558
[19] Kresse G and Furthmuller J 1996 *Phys. Rev.* B **54** 11169
[20] Kresse G and Furthmuller J 1996 *Comput. Mater. Sci.* **6** 15
[21] Perdew J P, Burke K and Ernzerhof M 1996 *Phys. Rev. Lett.* **77** 3865
[22] Kresse G and Joubert D 1999 *Phys. Rev.* B **59** 1758
[23] Monkhorst H J and Pack J D 1976 *Phys. Rev.* B **13** 5188
[24] Himpsel F J *et al* 1988 *Phys. Rev.* B **38** 6084